

## Charge-density-wave pinning and metastable-state dynamics in NbSe<sub>3</sub>

I. D. Parker\* and A. Zettl

*Department of Physics, University of California at Berkeley, Berkeley, California 94720*

(Received 13 September 1991)

We have explored transient charge dynamics associated with metastable pinning configurations in both charge-density-wave (CDW) states of NbSe<sub>3</sub>. The amount of charge associated with the pinned metastable states is less than  $10^{-5}$  of the total condensed CDW carrier density. Depinning the CDW results in a transient dynamics with corresponding charge mobilities of the order of  $10^6$  cm<sup>2</sup>/V sec, the highest mobility observed for any metallic conductor. At high temperatures in the CDW state, the transient response appears to be correlated with the CDW impurity-pinning strength. At low temperatures ( $T < 40$  K), this correlation breaks down, suggesting a sudden and dramatic change in the CDW-impurity interaction strength or, alternatively, a change in the effective CDW carrier density.

Charge-density-wave (CDW) dynamics in low-dimensional conductors has been the subject of intensive study over the past 15 years. The prototype material NbSe<sub>3</sub> shows two distinct CDW states, where the condensed electrons can be made to move or "slide" under the influence of a relatively small bias field  $E > E_T$ , where  $E_T$  is the threshold field needed to overcome an intrinsic pinning potential. Although it is generally accepted that the pinning of the CDW is due to random distribution of impurities within the specimen, the exact nature of the CDW-impurity interaction, including the temperature dependence of  $E_T$ , is controversial. Both thermal activation<sup>1</sup> and zero-temperature "effective-charge" models<sup>2</sup> have been proposed to account for  $E_T(T)$ .

Because of internal degrees of freedom of the CDW condensate and the interaction with impurities, the pinned state is not unique, but may assume different metastable configurations, depending upon the electrical and thermal history of the specimen. A dramatic manifestation of the metastable states in NbSe<sub>3</sub> (and related CDW conductors such as TaS<sub>3</sub>) is the so-called "pulse-sign memory" effect, where the transient CDW response to a rapidly applied bias field,  $E > E_T$ , is sensitive to the direction of the CDW motion during the previous depinning.<sup>3</sup> If the CDW was previously depinned in the opposite direction, a transient excess current appears, suggestive of a release of "stored" charge. Different metastable states are assumed to correspond to different local CDW phase configurations.

We have used the pulse-sign memory effect to investigate CDW pinning and transient dynamics in both CDW phases of NbSe<sub>3</sub>. In the upper CDW state ( $T < 144$  K), the temperature dependence of the charge associated with the metastable pinning states correlates with the strength of the (weak) impurity pinning. In the lower CDW state ( $T < 59$  K), we observe a sharp transition near 45 K, below which the metastable state configurations or the coupling of the CDW to the external field is dramatically altered. Below 40 K, no pulse-sign memory effect is seen. In both CDW states, the actual charge associated with the pinned metastable states

is only of the order  $10^{-5}$  of the total condensed carrier concentration. The carrier mobility achieved immediately after depinning can be in excess of  $10^6$  cm<sup>2</sup>/V sec, higher than for any other metallic conductor.

High-purity NbSe<sub>3</sub> samples with residual resistance ratios  $> 200$  and (lower CDW state) threshold field minima  $\sim 9.5$  mV/cm were used throughout this study. Typical sample dimensions were  $1 \text{ mm} \times 20 \text{ } \mu\text{m} \times 5 \text{ } \mu\text{m}$ , with resistances around  $50 \text{ } \Omega$  at room temperature. A four-probe configuration was used for dc resistance and threshold field measurements, while a two-probe configuration was used for the transient response measurements to minimize contact pinning effects. The pulse-sign memory effect was observed using a conventional drive and detection circuit. A train of rectangular,  $100\text{--}200\text{-}\mu\text{s}$ -wide current pulses was passed through the sample and the voltage response monitored on a 1-MHz bandwidth oscilloscope. A typical pulse train consisted of two positive, followed by two negative pulses, all with the same duration and magnitude, and each separated by  $100 \text{ } \mu\text{s}$  of dead time (during which the applied current was zero). The sequence was repeated at 45 Hz, low enough to avoid sample heating problems. The repetition rate of the pulse train was found to have no influence on the form or magnitude of the transient. To increase the sensitivity of the experiment, the Ohmic part of the voltage response was nulled out using a passive bridge circuit balanced to the Ohmic sample resistance well below threshold.

Figure 1 shows the threshold field  $E_T$  for nonlinear conduction as a function of temperature for a typical NbSe<sub>3</sub> sample. The functional form obtained for  $E_T$  is consistent with the results of many previous studies, and representative of the behavior corresponding to reasonably "thick" NbSe<sub>3</sub> samples, i.e., specimens in the three-dimensional limit. The upper CDW state displays a minimum value for  $E_T$  of 60 mV/cm near 115 K, while the lower CDW state shows a minimum value of  $\sim 10$  mV/cm at 48 K. In the temperature range between 57 and 46 K, independent depinnings of the two coexisting CDW's are observed.

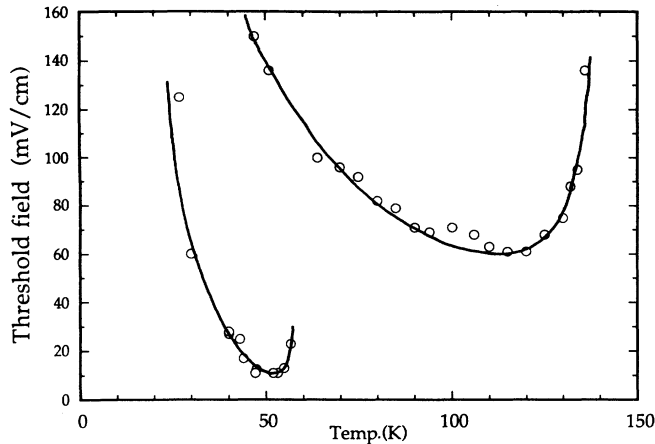


FIG. 1. Temperature dependence of the threshold field  $E_T$ . Open circles indicate data points and the solid line indicates the fit to the weak-pinning model given in the text.

The pulse-sign memory effect, identified as a transient voltage response whenever the polarity of the drive current pulse changes, is observed in both the upper and lower CDW states. The inset to Fig. 2 shows schematically the behavior of the bridge circuit output as seen on the oscilloscope. The transient peak represents excess current carried by the CDW, beyond that normally transported by the sliding CDW under steady-state dc drive conditions. We have attempted to quantify the transient behavior as a function of the field strength  $E$  and the temperature  $T$ . The precise functional form of the time-dependent transient current  $I_t(t; E, T)$  is difficult to extract directly because of the superimposed narrow-band

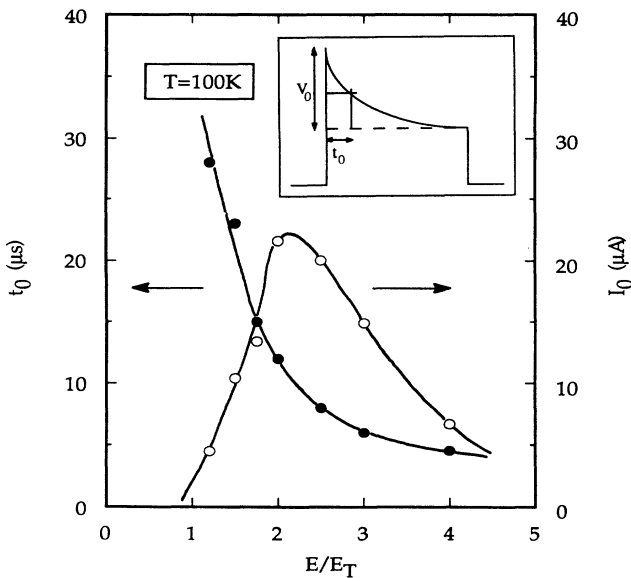


FIG. 2. The field dependence of the initial transient current excess  $I_0$  (open circles), and the decay time of the transient current  $t_0$  (filled circles), for the upper CDW at 100 K. The inset shows the form of the transient at the output of the bridge circuit, and indicates how  $I_0$  and  $t_0$  are derived. Note that narrow-band noise, normally superimposed onto the transient, is not indicated in this figure.

noise oscillations on the response wave form (these noise oscillations are not shown on the inset to Fig. 2). However, we may unambiguously identify two parameters which characterize the transient response:  $V_0$ , the excess transient voltage extrapolated to time  $=0$  (i.e., the start of the pulse on which the transient rides), from which we derive  $I_0$ , the excess transient current by dividing by the Ohmic resistance measured well below  $E_T$ ; and  $t_0$ , the time taken for the transient current excess to decay to one-half of its initial value.

Figure 2 shows how  $I_0$  and  $t_0$  vary as the  $E$  field is increased above the threshold field, for the upper CDW state at 100 K. (It should be noted that a small transient effect was noted even for fields slightly below  $E_T$ .) As  $E$  increases,  $t_0$  monotonically decreases, but  $I_0$  rises to a maximum near  $2E_T$  before decreasing. A similar behavior was found at all temperatures in both CDW states where the transient effect was seen. Unless otherwise noted, all data sets referred to in the remainder of this paper have been obtained using an electric field of  $E(T) = 1.5E_T(T)$ , a value for which both  $I_0$  and  $t_0$  are close to one-half of their maximum value.

Figure 3 shows the temperature dependence of the quantities  $t_0$  (upper curve) and  $I_0$  (lower curve). In the upper CDW state transient response is observed between 137 and 60 K, while for the lower CDW state transient response is observed between 57 and 40 K. It is interesting to note that while in the upper CDW state transient

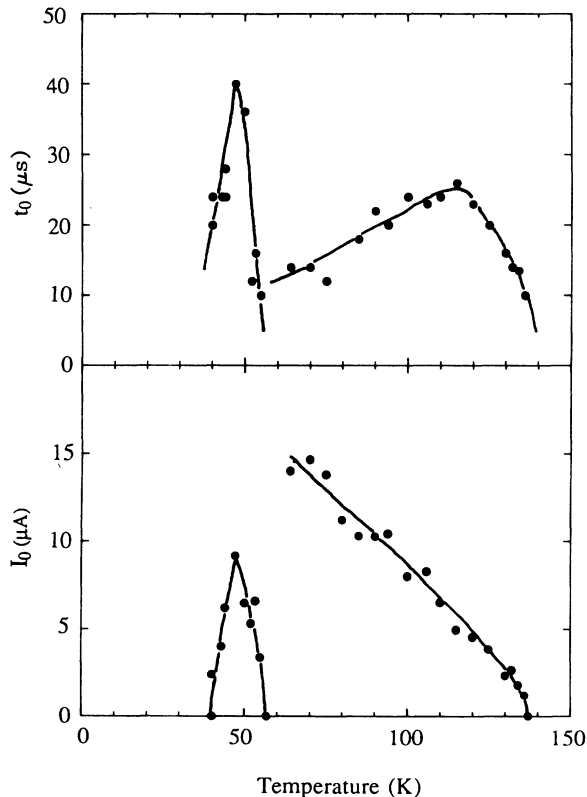


FIG. 3. The temperature dependence of the decay time  $t_0$  (upper figure) and the initial excess transient current  $I_0$  (lower figure).

response is obtained over nearly the whole temperature range between the upper and lower CDW transition temperatures, in the lower CDW state transient behavior occurs only over a restricted temperature range. Below 40 K, no transient effect is observed, despite the presence of a well-established CDW and a clearly identifiable threshold in  $E_T$ .

We now discuss these results. It has been suggested that the pulse-sign memory effect and related phenomena<sup>4</sup> result from the relaxation of metastable configurations of the CDW.<sup>5</sup> A bias field pulse above threshold will cause the CDW to slide and deform in the direction of its motion because of the interaction with the random impurity potential. Some portions are more strongly pinned than others, leading to internal CDW strain fields. As the bias electric field is quickly reduced below threshold and the CDW repins, the CDW relaxes back to the nearest metastable pinning configuration, which in general is not its true equilibrium ground state. The pinned metastable state is then in a state of "built-in" CDW polarization. When the polarity of the bias field reverses and depins the CDW, this built-in polarization "unwinds," giving rise to the excess current. The excess current is given by  $I_t(t) = \partial P / \partial t$ , where  $P$  is the instantaneous polarization of the CDW. For a bias pulse with the same polarity as the previous pulse, no excess current is seen, since the polarization is not released.

An important question is to what degree the CDW is polarized in a given metastable state. An estimate of the net initial CDW deformation is given by  $P_0 = I_0 t_0$ . Figure 4 shows (as open symbols)  $P_0$  plotted against temperature for both CDW states. In the upper CDW state (circles)  $P_0$  increases with decreasing temperature reaching  $\sim 150$  pC at 70 K. In the lower CDW state (triangles),  $P_0$  displays a sharp maximum of  $\sim 300$  pC near 45 K,

and a decrease to zero near 40 K. Although the spatial structure of the metastable polarization state is without doubt rather complicated, we can roughly associate  $P_0$  with the total CDW carrier density associated with the metastable states,  $n_{ms}$ . Taking a value for the total condensed carrier concentration  $n_c \sim 10^{21} \text{ cm}^{-3}$  in the upper CDW at 80 K, we find (using the value of  $P_0 \sim 150$  pC and the crystal dimensions) that  $n_{ms}/n_c \sim 10^{-5}$ , i.e., only about  $10^{-5}$  of the total CDW charge is associated with metastable states. This simple calculation assumes that the spatial structure of the polarization is uncomplicated, and that ignores the "backflow" of normal electrons, to balance the charge from the relaxing polarization. However, it probably gives a rough estimate of the degree of state polarization frozen in by the impurity interaction.

For a steady-state sliding CDW, the condensed carrier mobility is comparable to that of the normal electrons, with  $\mu = 40 \text{ cm}^2/\text{V sec}$ . In sharp contrast, the CDW charges associated with the metastable state depolarization have a much higher mobility. Although the amount of charge associated with the transient current is small compared with the charge associated with the CDW, the actual current magnitude is initially of the order of 20% of the total current carried by the sliding CDW. This implies a very high initial mobility for the associated metastable state carriers of  $\sim 10^6 \text{ cm}^2/\text{V sec}$ . Such extreme values for mobility are generally found only for very pure semiconductors at low temperatures, not metallic conductors near 100 K, where a value of  $5000 \text{ cm}^2/\text{V sec}$  is more typical.

It is desirable to correlate the temperature dependence of  $P_0$  shown in Fig. 4 with the CDW pinning strength and effective CDW carrier density. Neglecting any temperature dependence of the CDW-impurity interaction and the interaction of the CDW with normal (uncon-

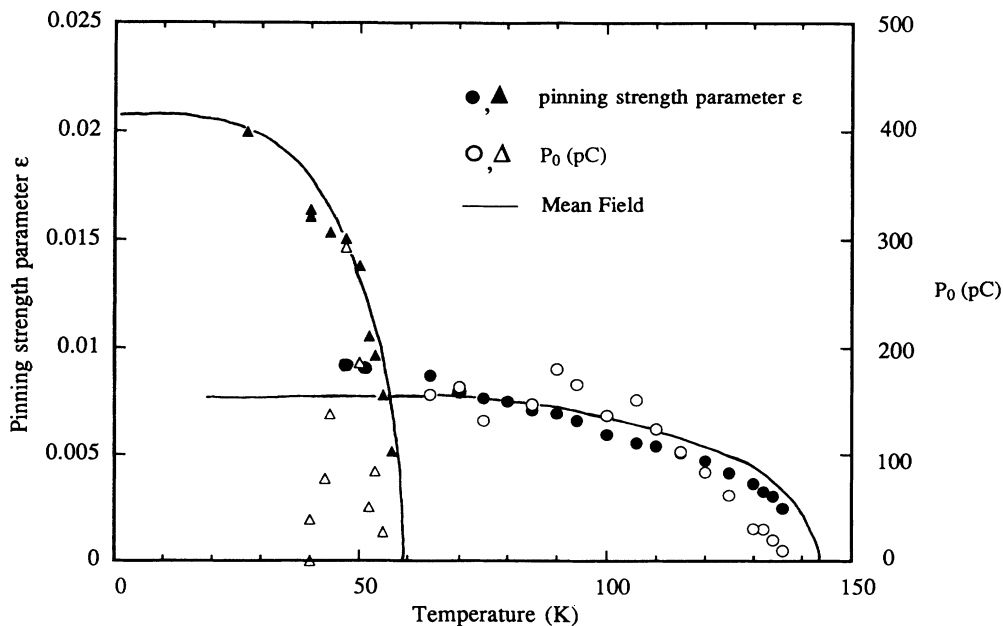


FIG. 4. Temperature dependence of the pinning strength parameter  $\epsilon$  (filled circles and triangles), and  $P_0 = I_0 t_0$  (open circles and triangles). Circles indicate data points for the upper CDW, while triangles indicate the lower CDW. The solid lines indicate mean-field behavior of the CDW order parameter (with an appropriate scaling factor, the same for both the upper and lower CDW).

densified) carriers, one might expect  $P_0$  to track the concentration of the condensed carriers,  $n_c$ . Near the CDW transition temperature,  $n_c$  is proportional to  $\Delta(T)$ , where  $\Delta$  is the CDW order parameter. Detailed x-ray scattering experiments in NbSe<sub>3</sub> show  $\Delta$  to be well described by mean-field behavior for both CDW states.<sup>6</sup> The solid lines in Fig. 4 show  $\Delta_1(T)$  and  $\Delta_2(T)$  for the upper and lower CDW states, respectively, assuming a mean-field behavior and using an appropriate scaling factor. Although the correspondence between  $\Delta$  and  $P_0$  seems reasonable for the upper CDW state and the lower CDW state above 45 K, there is a severe discrepancy in the lower CDW state below 45 K. It is interesting to note that other transport and magnetization studies on NbSe<sub>3</sub> have shown evidence for anomalous changes in the effective CDW carrier density in the same lower CDW state temperature range.<sup>7</sup>

Because the metastable pinned CDW configuration is intimately tied to the impurity-pinning potential, the pulse-sign memory effect should not only reflect the effective CDW carrier density but also the CDW-lattice interaction. Most models of CDW pinning and conduction are based on the Fukuyama-Lee-Rice (FLR) model,<sup>8,9</sup> in which a deformable CDW is pinned to the underlying lattice via phase fluctuations. The pinning strength may be categorized as either strong or weak. In strong pinning, the potential energy between the CDW and impurity dominates the strain energy associated with the local CDW distortion near the impurity; weak pinning corresponds to the opposite situation. In strong pinning, the CDW phase is fixed at each impurity site and CDW motion results in amplitude collapse (phase slip) at the impurity site. In weak pinning, the CDW phase is smoothly adjusted over many impurity sites to yield a collective pinning potential, and the CDW motion does not necessarily result in a complete local-amplitude collapse. In the FLR model, the temperature-dependent pinning strength parameter,  $\varepsilon(T)$ , is conveniently parametrized by

$$\varepsilon(T) = \frac{\rho_c V}{\Delta(T)}, \quad (1)$$

where  $\rho_c$  is the CDW carrier density and  $V$  is the impurity potential. In the strong-pinning regime  $\varepsilon \gg 1$ , while for weak pinning  $\varepsilon \ll 1$ .

The CDW-impurity interaction has been studied in some detail both experimentally and theoretically. In NbSe<sub>3</sub> nominal impurities of undoped crystals are believed to result in weak pinning. However many details of CDW pinning, such as the strength of the charged impurity atoms and the temperature dependence of  $E_T$  are still controversial.

Maki and Virosztek have recently proposed that  $E_T(T)$  can be accounted for by thermal fluctuations of the CDW phase.<sup>10</sup> In the weak-pinning limit they find

$$E_W(T) = E_W(0) \left[ \frac{\Delta(T)}{\Delta(0)} \frac{\rho}{\rho_c(T)} \exp \left[ \frac{-T}{T_0} \right] \right]^{4/(4-D)}, \quad (2)$$

where  $E_W(0)$  is the zero-temperature weak-pinning threshold field,  $\Delta(T)$  is the temperature-dependent CDW energy gap,  $\rho$  is the normal electron density,  $\rho_c$  is the CDW carrier density, the exponential term represents thermal fluctuations, and  $D$  is the dimensionality of the CDW.

Equation (2) provides good fits to  $E_T(T)$  for several different CDW materials, including NbSe<sub>3</sub>.<sup>10</sup> The solid lines in Fig. 1 show Eq. (2) fitted to the data of the NbSe<sub>3</sub> crystals discussed here. Excellent fits are obtained for both the upper and lower CDW states, with  $D=2$  (for both the upper and lower CDW), and  $T_0=65$  K,  $E_T(0)=558$  mV/cm for the upper CDW and  $T_0=13.5$  K,  $E_T(0)=3330$  mV/cm for the lower CDW. It should be noted that these values for  $D$  and  $T_0$  are very close to those found by other workers.<sup>11</sup> Maki and Virosztek have also proposed an expression for the temperature dependence of the threshold field in the strong-pinning limit.<sup>10</sup> This expression was found to fit the data much less successfully.

Combining Eqs. (1) and (2), with  $D=2$ , yields the pinning strength parameter  $\varepsilon(T)$  in the weak pinning limit:<sup>12</sup>

$$\varepsilon(T) = \left[ \frac{\rho^2 V^2}{\Delta(0)^2} \frac{E_W(0)}{E_W(T)} \exp \left[ \frac{-2T}{T_0} \right] \right]^{1/2}. \quad (3)$$

Tunneling studies have given values for  $\Delta(0)$  as 101 and 35 mV/cm for the upper and lower CDW, respectively.<sup>13</sup> Estimates of the CDW carrier density and the CDW pin-

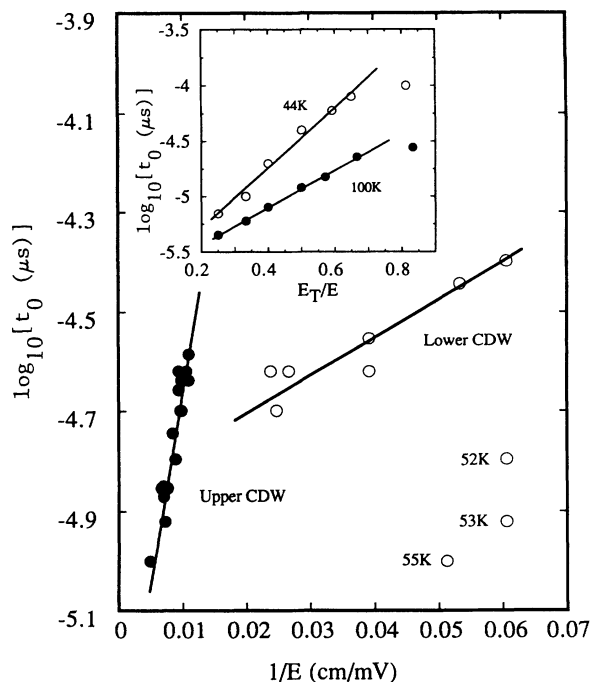


FIG. 5. (a)  $\log_{10}(t_0)$  vs  $E_T/E$  (where  $E$  is the bias across the sample) for the upper CDW at 100 K (filled circles) and the lower CDW at 44 K (open circles), as the bias  $E$  is varied above the threshold field. (b)  $\log_{10}(t_0)$  vs  $1/E$  for the upper CDW (filled circles) and the lower CDW (open circles) as the temperature is varied. Note that for all data points at temperature  $T$ , the electric field  $E$  has been adjusted to equal  $1.5E_T(T)$ .

ning energy density give  $\rho_c/\rho \sim 0.1$  and  $\rho_c V \sim 1$  meV at  $T=0$ .<sup>9</sup> Combining these, we derive an estimate of  $\rho V \sim 10$  meV. Assuming that  $\rho V$  is only weakly temperature dependent, Eq. (3) establishes  $\epsilon(T)$  from the measured  $E_T(T)$ . Values for  $\epsilon(T)$  thus determined are shown as solid symbols in Fig. 4. The magnitude of  $\epsilon$  is  $\ll 1$  which suggests weak pinning for both CDW states. This pinning strength is seen to increase with decreasing temperature for both CDW states. It is also found that, despite displaying a smaller value for  $E_T(T)$ , the lower CDW generally has a greater pinning strength, a consequence of its smaller energy gap. Figure 4 shows evidence that the metastable state pinning strength may correlate with the pinning strength, but only above 45 K. The sudden deviation of  $P_0$  from the calculated form of  $\epsilon$  in Fig. 4 suggests a sudden and dramatic breakdown of  $\rho_c V$  below this temperature.

Finally we discuss the decay rate of the polarization, defined here as  $t_0^{-1}$ . For a given fixed temperature,  $t_0$  decreases rapidly with increasing electric field  $E$ , as demonstrated in Fig. 2. Figure 5(a) shows  $\log_{20}(t_0)$  plotted against  $1/E$ , the data being obtained by fixing the temperature and varying  $E$ . The data fall on a line, indicating a functional form for the relaxation rate:

$$t_0^{-1} \propto \exp(-\text{const}/E). \quad (4)$$

Figure 5(b) shows similar data, obtained at various tem-

peratures in both CDW states. Each point in this figure corresponds to a different temperature, for which  $E$  was adjusted to be equal to  $1.5E_T(T)$ . The solid circles are for temperatures corresponding to the upper CDW state, while the open circles correspond to the lower CDW state. Again the data fall on a straight line consistent with the empirical expression Eq. (4). The three notable exceptions in Fig. 5(b) are for the temperatures corresponding to 52, 53, and 55 K. Interestingly, in this temperature range the two coexisting CDW's can be independently depinned (see Fig. 1). It is possible that in this temperature range the CDW deformations of the upper and lower CDW couple together and influence the relaxation rate. We also remark that no empirical relations of the form  $t_0^{-1} \sim \exp(-\text{const}/k_B T)$  were found, indicating that simple thermal activation is not the governing process for the transient decay.

In conclusion, the transient response in NbSe<sub>3</sub> has been used to extract the density and mobility of the CDW carriers associated with the metastable pinning configurations. Below 45 K, anomalous behavior is observed suggestive of a dramatic change in the CDW effective charge density or the CDW-impurity interaction strength.

This work was supported by NSF Grant No. DMR90-17254.

\*Present address: Cavendish Laboratory, Madingley Rd., Cambridge CB3 0HE, England.

<sup>1</sup>K. Maki, Phys. Rev. B **33**, 2852 (1986); K. Maki and A. Virosztek, *ibid.* **42**, 655 (1990).

<sup>2</sup>J. McCarten, M. Maher, T. L. Adelman, D. A. Dicarlo, and R. E. Thorne, Phys. Rev. B **43**, 6800 (1991).

<sup>3</sup>J. C. Gill, Solid State Commun. **39**, 1203 (1981).

<sup>4</sup>G. Mihaly and L. Mihaly, Phys. Rev. Lett. **52**, 149 (1984); J. Dumas and C. Schlenker, Solid State Commun. **45**, 885 (1983). See also, for example, *Charge Density Waves in Solids*, edited by G. Hutiray and J. Solymon, Lecture Notes in Physics Vol. 27 (Springer, Berlin, 1985), particularly J. Dumas and C. Schlenker (p. 439); N. P. Ong, D. D. Duggan, C. B. Kalem, and T. W. Jing (p. 387), A. Jánossy, G. Mihaly, and L. Mihaly (p. 412).

<sup>5</sup>P. Littlewood and R. Rammal, Phys. Rev. B **38**, 2675 (1988); A. Erzan, E. Veermans, R. Heijungs, and L. Pietronero, *ibid.* **41**, 11 522 (1990).

<sup>6</sup>R. M. Flemming, D. E. Moncton, and D. B. McWhan, Phys. Rev. B **18**, 5560 (1978).

<sup>7</sup>N. P. Ong and P. Monceau, Solid State Commun. **26**, 487 (1978); R. V. Coleman, G. Eiserman, M. P. Everson, and A. Johnson, Phys. Rev. Lett. **55**, 863 (1985); P. Monceau and J.

Richard, Phys. Rev. B **37**, 7982 (1988); I. D. Parker and A. Zettl (unpublished data), showing a significant enhancement of the magnetothermopower in NbSe<sub>3</sub> below 35 K in magnetic fields  $\sim 1$  T and further data showing significant reduction ( $\sim 50\%$ ) of the lower CDW depinning threshold field below 35 K for NbSe<sub>3</sub> in magnetic fields ( $< 8$  T).

<sup>8</sup>H. Fukuyama, J. Phys. Soc. Jpn. **41**, 513 (1976); H. Fukuyama and P. A. Lee, Phys. Rev. B **17**, 535 (1977).

<sup>9</sup>P. A. Lee and T. M. Rice, Phys. Rev. B **19**, 3970 (1979).

<sup>10</sup>K. Maki and A. Virosztek, Phys. Rev. B **39**, 9640 (1989).

<sup>11</sup>In Ref. 10, Maki and Virosztek find  $D=2$  for both upper and lower CDW, with  $T_0=60.6$  K (upper CDW) and 14.6 K (lower CDW). Coleman *et al.* find  $T_0=15.2$  K (lower CDW); R. V. Coleman, M. P. Everson, G. Eiserman, and A. Johnson, Phys. Rev. B **32**, 537 (1985).

<sup>12</sup>It should be noted that although Eq. (2) provides an excellent fit to the  $E_T(T)$  data, the thermal fluctuation model predicts parameter magnitudes in apparent conflict with those obtained from experimental studies of NbSe<sub>3</sub> samples of different sizes and impurity concentrations (Ref. 2). Hence, the validity of Eq. (2) and the consequent temperature dependence of  $\epsilon$  given by Eq. (3) are subject to some interpretation.

<sup>13</sup>Zhenxi Dai, C. G. Slough, and R. V. Coleman (unpublished).